

# Mapping brain morphological and functional conversion patterns in amnesic MCI: a voxel-based MRI and FDG-PET study

Silvia Morbelli · Arnoldo Piccardo · Giampiero Villavecchia · Barbara Dessi ·  
Andrea Brugnolo · Alessandra Piccini · Anna Caroli · Giovanni Frisoni ·  
Guido Rodriguez · Flavio Nobili

Received: 10 March 2009 / Accepted: 1 July 2009 / Published online: 7 August 2009  
© Springer-Verlag 2009

## Abstract

**Purpose** To reveal the morphological and functional substrates of memory impairment and conversion to Alzheimer disease (AD) from the stage of amnesic mild cognitive impairment (aMCI).

**Methods** Brain MRI and FDG-PET were performed in 20 patients with aMCI and 12 controls at baseline. During a mean follow-up of about 2 years, 9 patients developed AD

(converters), and 11 did not (nonconverters). All images were processed with SPM2. FDG-PET and segmented grey matter (GM) images were compared in: (1) converters versus controls, (2) nonconverters versus controls, and (3) converters versus nonconverters.

**Results** As compared to controls, converters showed lower GM density in the left parahippocampal gyrus and both thalami, and hypometabolism in the precuneus, posterior cingulate and superior parietal lobule in the left hemisphere. Hypometabolism was found in nonconverters as compared to controls in the left precuneus and posterior cingulate gyrus. As compared to nonconverters, converters showed significant hypometabolism in the left middle and superior temporal gyri.

**Conclusion** The discordant topography between atrophy and hypometabolism reported in AD is already present at the aMCI stage. Posterior cingulate–precuneus hypometabolism seemed to be an early sign of memory deficit, whereas hypometabolism in the left temporal cortex marked the conversion to AD.

S. Morbelli (✉)  
Nuclear Medicine Unit, Department of Internal Medicine,  
University of Genoa,  
Viale Benedetto XV, 6,  
16132 Genoa, Italy  
e-mail: silviadaniela.morbelli@hsanmartino.it

A. Piccardo · G. Villavecchia  
Nuclear Medicine Unit, Department of Radiology,  
Galliera Hospital,  
Genoa, Italy

B. Dessi · A. Brugnolo · G. Rodriguez · F. Nobili  
Clinical Neurophysiology Unit, Department of Neurosciences,  
Ophthalmology and Genetics, University of Genoa,  
Genoa, Italy

A. Piccini  
Cell Biology Unit, National Cancer Research Institute,  
Genoa, Italy

A. Caroli · G. Frisoni  
LENITEM - Laboratory of Epidemiology  
Neuroimaging & Telemedicine,  
IRCCS San Giovanni di Dio Fatebenefratelli,  
Brescia, Italy

A. Caroli  
Medical Imaging Unit, Biomedical Engineering Department,  
Mario Negri Institute,  
Bergamo, Italy

**Keywords** Brain PET · Alzheimer's disease ·  
Mild cognitive impairment · Voxel based morphometry ·  
Alzheimer's disease biomarkers

## Introduction

In the area of the early diagnosis of Alzheimer's disease (AD), research is very active in finding, defining and validating biomarkers that can detect the typical neurodegeneration of AD both in predementia stages, i.e. in mild cognitive impairment (MCI), and in screening of the high-risk asymptomatic population [1]. The development

of effective pharmacotherapy, aimed at altering the natural history of the disease from these earliest stages, requires the diagnosis of AD to be made with the highest accuracy [2].

Within the MCI group, patients who show an impairment in the memory domain (amnestic MCI, aMCI), either associated or not with a slight impairment in other cognitive areas [1, 2], are of particular interest because they have been proven to have a high risk of developing AD within a few years [3]. In aMCI patients, before a diagnosis of predementia AD becomes probable, the ‘core’ deficit in episodic memory [1, 4] must be supported by evidence of AD neurodegeneration through one or more ‘biomarkers’, such as brain volume loss (atrophy) on MRI, cortical hypometabolism on  $^{18}\text{F}$ -FDG PET in specific regions [4], and altered levels of  $\text{A}\beta$  1–42 amyloid and tau protein in the cerebrospinal fluid [1, 5]. Consistent with the profound cell loss in the hippocampal formation observed in pathological studies [6, 7], MRI ROI-based studies have demonstrated medial temporal lobe (MTL) atrophy in early-stage AD [8], as well as in MCI, involving the hippocampus, entorhinal cortex, amygdala and parahippocampal gyrus [9, 10]. Studies applying voxel-based morphometry (VBM) have identified similar patterns of MTL atrophy in aMCI, but have also highlighted regions of atrophy in the inferior and lateral temporal lobes, the cingulate gyrus, and the parietal and frontal lobes [11, 12].

While MRI findings generally match the topography of atrophy in pathological studies, cortical hypometabolism on FDG PET is more often found in the posterior cingulate, the parietal precuneus and the posterior temporoparietal regions and less frequently in the MTL [13]. Even if this mismatch might be partially due to the intrinsic limited spatial resolution of the earliest PET scanners [13], some pathophysiological explanations have also been addressed. Indeed, metabolic deficit in posterior cortical regions could be due to distant MTL pathology, since posterior cortical regions are densely interconnected with the MTL [14].

A critical issue is that the majority of studies have investigated either atrophy [12] or hypometabolism [15], while only a few [16–19] have used the two imaging modalities in the same group of patients. In fact, given the presence of large intersubject variability in the topography of the disease, studies using either MRI or PET alone are less adequate to clarify the presence and the neurophysiological meaning of dissociating or overlapping results. Some recent studies have involved the use of both VBM and FDG PET voxel-based analysis (VBA) in the same group of patients with early AD or MCI [16–18]. In one of these studies in MCI patients, Chetelat et al. [16] found a direct correlation between both encoding and retrieval memory scores and hippocampal grey matter (GM) density. Moreover, encoding was correlated with hippocampal

glucose consumption (CMRglc), whereas retrieval was correlated with the posterior cingulate CMRglc.

With the aim of concurrently investigating patterns of atrophy and hypometabolism in patients with aMCI converted to AD, we performed both VBM and PET VBA and compared subgroups of patients with aMCI converted (converters) or not converted (nonconverters) to AD with a group of healthy controls.

## Subjects and methods

### Patients

The study included 20 consecutive outpatients (11 women, 9 men; mean age  $76.0 \pm 5.5$  years, range 62–86 years) with memory complaints in whom an objective memory deficit was demonstrated by means of neuropsychological tests. These patients came from one of the outpatient clinical units for the diagnosis and treatment of cognitive disorders at our university hospital. This clinical unit is part of the European Alzheimer Disease Consortium (EADC), joining centres of excellence across Europe and promoting clinical research in the dementia field. Some of the patients came from the EU-funded multicentric ‘DESCRIPA’ study, aimed at developing screening guidelines and clinical criteria for predementia AD [20], of which the functional neuroimaging substudy was a spontaneous part.

Dementia was excluded on the basis of clinical interview with both patients and caregivers using the Mini-Mental State Examination (MMSE) [21] for general cognition, questionnaires for Activities of Daily Living (ADL) [22] and instrumental ADL (IADL) [23], and the Clinical Dementia Rating (CDR) scale, that was 0.5 in all patients. Patients underwent a standard battery of blood count, blood chemical examinations and urinalysis, according to commonly followed rules to exclude secondary causes of cognitive impairment. The presence of analphabetism, major visual disturbance, psychiatric illness, epilepsy, major head trauma, Parkinsonism, previous stroke or TIA, and brain masses were further exclusion criteria. A mild depressive trait, as ascertained by the 15-item Geriatric Depression Scale (GDS), was not considered an exclusion criterion. Neuropsychiatric symptoms were assessed by interviewing the informant using the Neuropsychiatric Inventory (NPI) [24]. Patients scoring higher than 0 on the delusion and hallucination NPI items were excluded.

Patients underwent a neuropsychological test battery, including evaluation of (1) verbal episodic memory (immediate and delayed recall, IR and DR respectively) by the six-trial selective reminding test (SRT) [25], (2) visuomotor abilities, divided and attentional shifting by the Trail-making test, forms A (TMT-A) and B (TMT-B), (3)

categorical verbal fluency (2' test for animals), (4) visuoconstructional abilities by the copying figures test, including simple copy and copying with guiding landmarks of the mental deterioration battery [26], (5) abstract and logical reasoning by the Raven's PM38 matrices (set A–D, according to Spinnler and Tognoni [27]), and (6) executive attention by the Stroop colour-word test (correct items achieved in 30 s, according to Barbarotto et al. [28]). The clock completion test (as evaluated according to Watson et al. [29]) was used as a mixed measure of visuospatial abilities and executive functions, and the symbol-digit test [30] as a mixed measure of working memory and executive functions.

Any z-score lower than  $-1.5$ , based on the pertinent normative database and corrected for age and education, denoted impairment in a specific cognitive domain. According to Petersen's criteria [1], patients with a z-score lower than  $-1.5$  in either SRT IR or DR were considered as aMCI. Multi- or single-domain aMCI was defined according to the presence or absence of z-scores lower than  $-1.5$  in any of the other cognitive domains, respectively.

All patients were carefully treated for systemic comorbidity; drugs known to depress brain synaptic transmission, such as benzodiazepines and tricyclic antidepressant, were withdrawn. After the baseline examination, patients underwent clinical follow-up (including MMSE, ADL and IADL questionnaires, and CDR) every 6 months. A follow-up time of at least 1 year was available in all patients. During the follow-up (mean time  $23.5 \pm 10.1$  months), 9 patients developed dementia of the AD type (converters), according to the NINCDS-ADRDA [31] and DSM-IV criteria, while 11 patients were confirmed to have aMCI (nonconverters). Five converters showed only a memory deficit (single-domain aMCI), and four also showed deficit in other cognitive domains (multidomain aMCI), including the TMT-B (all four patients), the symbol digit test and the Stroop colour-word test (both tests in the same two

patients). Among the nonconverters, four had single-domain aMCI, and seven had multidomain aMCI, showing a deficit also in the TMT-A (four patients), TMT-B (four patients), the symbol digit test (five patients), the constructional apraxia test with guiding landmarks (four patients), and the Stroop colour-word test (one patient). All patients gave their informed consent to participate in the study.

## Controls

The protocol received the approval of the local ethics committee. Control subjects were healthy volunteers giving their informed consent, recruited during university courses dedicated to elderly people. Their health was carefully checked by means of general medical history, clinical examination and the same exclusion criteria as for the patients, with the exception of cognitive complaints. MMSE was performed and only subjects with a normal score (i.e.  $>26$ ) were further considered. Moreover, only subjects with a CDR of 0 were included. Healthy subjects underwent the same neuropsychological battery of tests as the patients, and only subjects with normal scores ( $Z > -1.5$ ) in all tests were further considered. After exclusion of 4 subjects in whom MRI scan could not be performed due to metallic devices or claustrophobia, 12 subjects (4 men and 8 women; mean age  $70.6 \pm 7.1$  years, range 62–83 years) were finally included in the study. Control subjects were asked to undergo continued evaluation to confirm their normal status over time.

Table 1 shows the main baseline demographics and both baseline and follow-up MMSE scores of the three groups of subjects (12 controls, 11 nonconverters, and 9 converters).

## PET data acquisition and preprocessing

PET was performed within 3 months from the baseline clinical-neuropsychological examination (mean 29.9 days

**Table 1** Main baseline demographic and clinical features of the three groups, as identified at follow-up

	Normal controls	aMCI converters	aMCI nonconverters
Number	12	9	11
Age (years)	$70.4 \pm 7.3$	$77.1 \pm 5.9^*$	$74.0 \pm 5.3^*$
Sex (M/F)	2/10	2/7	6/5
Education (years)	$10.6 \pm 4.5$	$8.6 \pm 4.3$	$8.7 \pm 4.5$
Follow-up time (months)	$22.3 \pm 10.5$	$22.6 \pm 10.7$	$26.5 \pm 11.3$
MMSE score			
Baseline	$28.7 \pm 1.3$	$27.8 \pm 0.9$	$27.8 \pm 1.4$
Follow-up	$28.9 \pm 1.1$	$24.6 \pm 2.0^*$	$27.0 \pm 2.7^*$
Recall <sup>a</sup>			
Immediate	$35.8 \pm 10.1$	$24.3 \pm 1.5^*$	$27.1 \pm 4.3^*$
Delayed	$5.4 \pm 2.7$	$1.1 \pm 0.9^*$	$2.1 \pm 1.1^*$
ApoE genotype	n.a.	3/7 (43%) <sup>b</sup>	2/6 (33%) <sup>b</sup>

\* $p < 0.05$ , converters and nonconverters versus normal controls.

<sup>a</sup> Buschke-Fuld selective reminding test.

<sup>b</sup> ApoE genotype was available only in seven converters and six nonconverters.

in patients and 29.8 days in controls). Subjects fasted for at least 6 h. Before radiopharmaceutical injection, blood glucose was checked and was <140 mg/dl in all subjects. After 10 min rest in a silent and darkened room, with eyes closed and ears unplugged, subjects were injected with approximately 370 MBq of  $^{18}\text{F}$ -FDG via a venous cannula, according to the guidelines of the European Association of Nuclear Medicine [32]. They remained in the room for 30 min after the injection, then they were moved to the PET room where scanning started approximately 45 min after injection and lasted for 20 min. A polycarbonate head holder was used to reduce head movements during the scan. Images were acquired using a Discovery ST PET-CT system (GE Healthcare, USA) on a  $128 \times 128 \times 64$  matrix (isotropic voxel of 2.34 mm) in two-dimensional mode with a total axial field of view of 15 cm and no interplane gap space. Images were reconstructed using an OSEM algorithm, 16 subsets and two iterations. Dicom files were exported and converted to Analyse files.

PET scans were normalized to the standard space described by Talairach and Tournoux [33] using the SPM2 package (Wellcome Department of Cognitive Neurology, London, UK) [34] running on Matlab 6.5 (Mathworks, Natick, MA). Since it was shown that the use of the standard  $^{15}\text{O}$ - $\text{H}_2\text{O}$  PET template provided with the SPM package to normalize FDG PET scan may generate inconsistent results [35], a fully MRI-based normalization was applied [36]. Each FDG PET scan was first coregistered to the pertinent MRI scan (six parameters, rigid body transformation) using the coregistration algorithm available in the SPM2 package. Each MR image was then spatially normalized to the SPM2 T1-MRI template using an affine plus nonlinear transformation, and the resulting deformation field was applied to the coregistered FDG PET scan. The spatially normalized PET images were finally smoothed with a 10-mm isotropic gaussian filter to blur individual variations in gyral anatomy and to increase the signal-to-noise ratio.

### MRI acquisition and preprocessing

All MRI volumes were obtained using 1.5-T superconductive system (Gyrosan Intera, Philips Medical Systems, Best, The Netherlands) to acquire a sagittal T1-FFE sequence with the following parameters: TR 8.7 ms, TE 4.1 ms, flip angle  $8^\circ$ , FOV 256 mm, matrix  $256 \times 256$ , 150 sagittal slices (1.0-mm thick), and voxel size  $0.98 \times 0.98 \times 1.6$ . MR images were obtained 0–28 days before PET examination.

Images were preprocessed with SPM2, using a modified optimized VBM technique following the method of Good et al. [37]. First, a customized sample-specific whole-brain template was computed, and a priori maps for GM, white matter, and cerebrospinal fluid were determined by segmenting the sample-specific whole-brain template into

the three components based on image intensity classification and probability of tissue class membership. Each individual MR scan was normalized to the whole-brain sample-specific template and then segmented into GM, white matter, and cerebrospinal fluid components using information from the sample-specific tissue classification templates. The individual GM images were further spatially normalized to the sample-specific GM template using a 12-parameter affine transformation and nonlinear adjustments with  $7 \times 8 \times 7$  basis functions. The segmented, normalized images were finally smoothed with an 8-mm full-width half-maximum gaussian kernel in order to compensate for inter-individual variability and conform the data to a gaussian distribution to enable the use of the random field theory which provides for corrected statistical inference.

### Statistical analysis

To fully explore GM loss and metabolic patterns related to aMCI and conversion to AD, PET and GM images from of aMCI patients were compared on a voxel-by-voxel basis to those from the normal controls using ANCOVA. Age, gender and years of education were included in the analysis as confounding variables. For both PET and GM images, the following comparisons were performed: (1) converters versus controls, (2) nonconverters versus controls, and (3) converters versus nonconverters. SPM-T maps were displayed using an uncorrected  $p < 0.005$  height threshold. This more liberal choice was adopted to avoid type II errors attributable to over-conservative thresholds [38]. In fact, considering the relatively low sensitivity of PET without repeated measures, higher thresholds could lead to false-negative results in PET studies. Clusters of differences were regarded as significant if they survived the  $p < 0.005$  threshold, corrected for multiple comparisons at cluster level. Only significant clusters containing at least 40 (VBM) or 100 (PET VBA) voxels were taken into consideration.

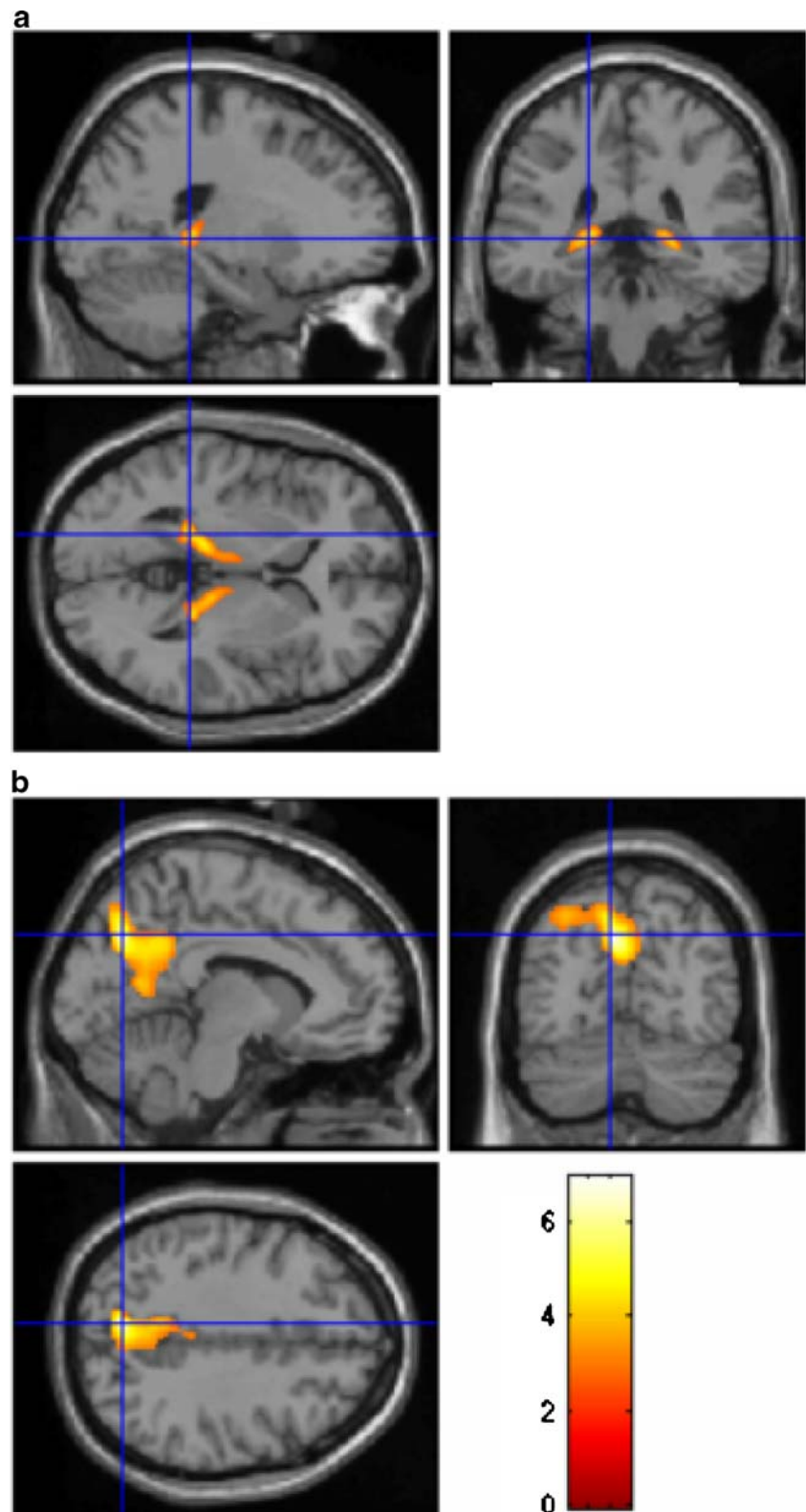
## Results

### GM density and hypometabolism patterns

*Converters versus controls* As compared to controls, converters showed reduced GM density in the left parahippocampal gyrus and the bilateral thalamus (Fig. 1a, Table 2), and relative hypometabolism in a region including left precuneus, posterior cingulate and superior parietal lobule (Fig. 1b, Table 2).

*aMCI Nonconverters vs normal controls* No significant GM reduction was found in nonconverters as compared to

**Fig. 1** Comparison between converters and controls in terms of GM density (**a**) and FDG uptake (**b**). For both comparisons, the height threshold of significance was set at  $p < 0.005$  uncorrected (voxel level) and at  $p < 0.05$  corrected for multiple comparisons (cluster level). Regions of significant difference are shown colour-graded in terms of Z values. Converters showed reduced GM density in a region including the left parahippocampal gyrus and bilateral thalamus (**a**) and hypometabolism in a posterior region including the left precuneus, posterior cingulate and superior parietal areas (**b**). Talairach coordinates and further details are available in Table 2



controls. On the other hand, nonconverters showed significant relative hypometabolism in a region including the left precuneus and the left posterior cingulate gyrus (Fig. 2, Table 2).

*Converters versus nonconverters* As compared to nonconverters, converters showed significant relative hypometabolism in the left middle and superior temporal gyri and no significant GM reduction (Fig. 3, Table 2).

**Table 2** Results of the comparison between controls, converters and nonconverters to AD in terms of both GM density (GM VBM) and FDG uptake (PET VBA)

Comparison	Analysis	Cluster level			Voxel level			
		Cluster extent (no. of voxels)	Corrected <i>p</i> value	Cortical region	Maximum Z score	Talairach coordinates	Cortical region	Brodmann area
Converters vs controls	GM VBM	7,836	0.0001	Left limbic lobe	5.02	-17, -36, 5	Parahippocampal gyrus	30
				Left thalamus	3.97	-15, -29, 4	Thalamus	
				Right thalamus	3.92	20, -32, 4	Thalamus	
	PET VBA	2,085	0.0001	Left parietal	4.78	-8, -66, 38	Precuneus	7
				Left parietal	3.72	-33, -62, 49	Superior parietal lobule	7
				Left limbic lobe	3.37	-8, -49, 13	Posterior cingulate gyrus	29
Nonconverters vs controls	PET VBA	941	0.001	Left limbic lobe	3.60	-4, -49, 23	Posterior cingulate gyrus	23
				Left parietal	3.53	0, -62, 33	Precuneus	7
Converters vs nonconverters	PET VBA	800	0.03	Left temporal	3.91	-51, 1, -24	Middle temporal gyrus	21
				Left temporal	3.11	-53, -20, -19	Middle temporal gyrus	21
				Left temporal	3.09	-40, 1, -15	Superior temporal gyrus	38

Uncorrected  $p < 0.005$  at the voxel level and  $p < 0.05$  corrected for multiple comparisons at the cluster level were accepted as statistically significant.

**Fig. 2** Comparison between nonconverters and controls in terms of FDG uptake. The height threshold of significance was set at  $p < 0.005$  uncorrected (voxel level) and at  $p < 0.05$  corrected for multiple comparisons (cluster level). Regions of significant difference are shown colour-graded in terms of Z values. Nonconverters showed significant hypometabolism in a region including the left precuneus and the left posterior cingulate gyrus. Talairach coordinates and further details are available in Table 2

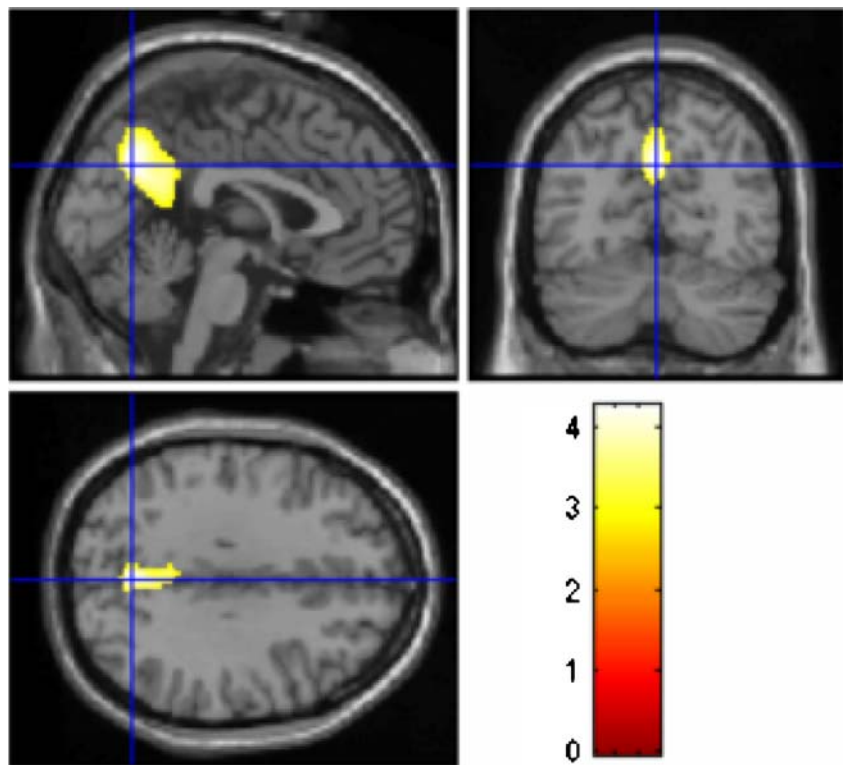
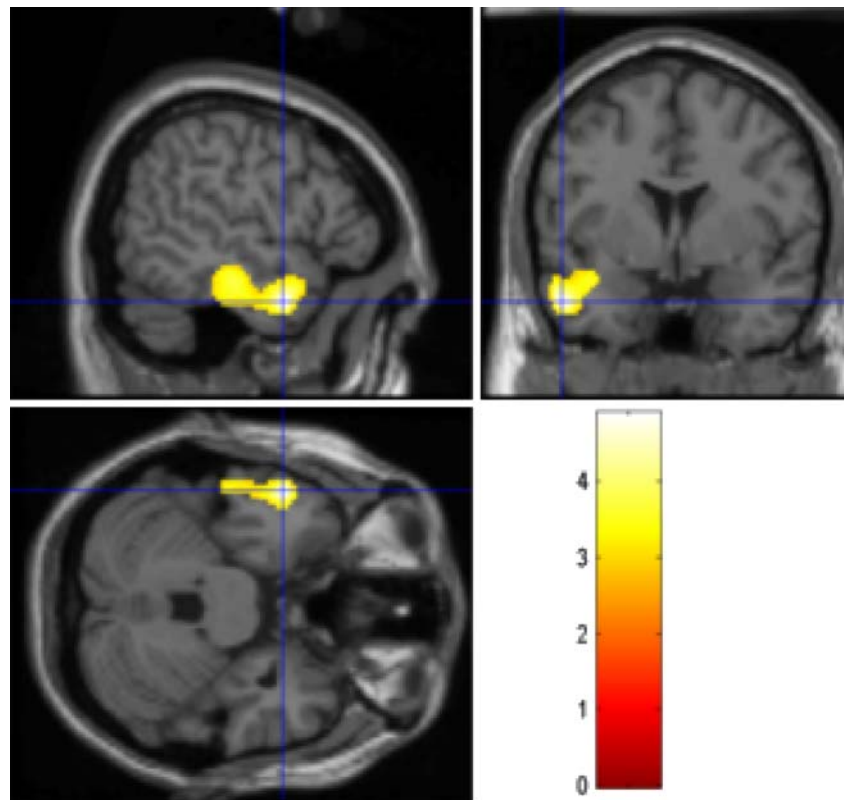


**Fig. 3** Comparison between converters and nonconverters in terms of FDG uptake. The height threshold of significance was set at  $p < 0.005$  uncorrected (voxel level) and at  $p < 0.05$  corrected for multiple comparisons (cluster level). Regions of significant difference are shown colour-graded in terms of Z values. Compared to nonconverters, converters showed significant relative hypometabolism in the left middle and superior temporal gyri. Talairach coordinates and further details are available in Table 2



#### Post-hoc analysis

Converters showed a significant relative hypometabolism in the left middle and superior temporal gyri as compared to nonconverters; however, such hypometabolism was not found in the comparison between converters and controls. To further explore the pathophysiological meaning of this finding, we tested the hypothesis of relatively higher metabolic values within these regions in nonconverters as compared to controls. Therefore, a post-hoc analysis was performed, using the same parameters used for previous analysis. Compared to controls, nonconverters showed a relative hypermetabolism in the left middle and superior temporal gyri (Fig. 4).

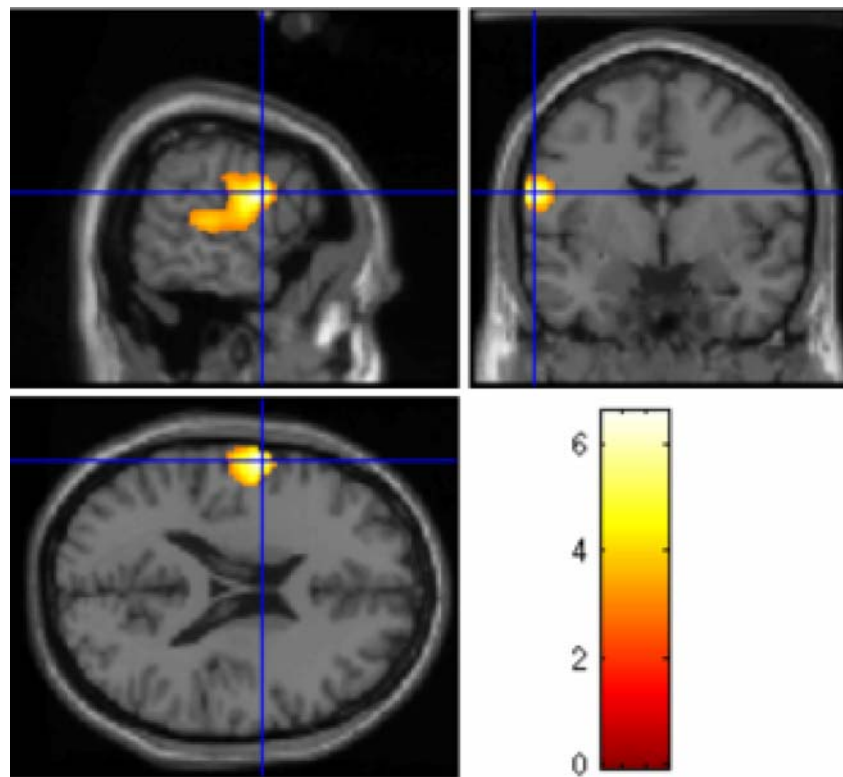
#### Discussion

The finding of posterior cingulate and precuneus hypometabolism in aMCI is in keeping with previous observations concerning both MCI [39] and very early AD [40]. A partially overlapping posterior cingulate/precuneus hypometabolism pattern was found in both converters and nonconverters as compared to controls. Although the significance of posterior cingulate hypometabolism was higher in converters than in nonconverters, as compared to controls, direct comparison between converters and nonconverters did not yield further significant cingulate

hypometabolism in converters. This could have been due to the small sample size. However, as posterior cingulate hypometabolism was found in both converters and nonconverters, it appears to be an early sign of memory deficit rather than a specific hallmark of AD conversion. This finding is in line with previous studies. Nestor et al. [39] have suggested that significant hypometabolism in the posterior cingulate is typical of all MCI patients, without a direct relationship to their future conversion. In a recent SPECT study, aMCI converters and nonconverters were found to share a common retrosplenial pattern of hypoperfusion [41], suggesting that retrosplenial cortex dysfunction could be the pathophysiological correlate of memory impairment, without being a biomarker of conversion to dementia. Although the group of nonconverters might have included some late converter patients due to the limited follow-up time, the risk of AD conversion is at a maximum within the first few years following the diagnosis of aMCI, and then substantially decreases [42]. FDG PET long-term follow-up studies in stable aMCI are needed to show whether posterior cingulate hypometabolism is confirmed over time despite the lack of dementia or whether subjects with hypometabolism in this region convert to AD-type dementia over longer follow-up intervals.

GM VBM highlighted neuronal loss in the left parahippocampal gyrus in converters as compared to controls. This result is in agreement with previous structural MRI

**Fig. 4** Post-hoc comparison between nonconverters and controls in terms of FDG uptake. The height threshold of significance was set at  $p < 0.005$  uncorrected (voxel level) and at  $p < 0.05$  corrected for multiple comparisons (cluster level). Regions of significant difference are shown colour-graded in terms of Z values. Compared to controls, nonconverters showed relative increased metabolism in the left middle and superior temporal gyri



studies and with the topographical progression of neurofibrillary pathology, which begins in the MTL structures and progresses to paralimbic, basal temporal and other neocortical association areas [43]. On the basis of these imaging/pathology correlation studies, quantitative measures from structural MRI are generally considered to represent a surrogate measure of the stage/severity of neuronal pathology that occurs in AD.

The topographical mismatch between MRI/pathology and PET results may be explained in terms of AD disconnection syndrome, as both the precuneus and posterior cingulate are densely interconnected with the hippocampus and parahippocampal region [44]. PET measurements of glucose consumption reflect local baseline integrated synaptic activity and therefore are mainly sensitive to synaptic dysfunction rather than to neuronal loss [45], while VBM assesses structural changes only. Neuropathological studies have shown that degeneration of neuronal synapses and neuronal processes, and the shrinkage of neuronal cell bodies of neurons, may precede the death and elimination of neurons in AD for a substantial period [46].

Besides MTL atrophy, converters also showed bilateral thalamic atrophy, in comparison with controls. Reduced GM density in AD has already been found using VBM analysis within thalamic structures. In particular, Callen et al. [47] found that the limbic system as a whole shows significant atrophy in patients with AD, in agreement with previous neuropathological studies showing that neurofi-

brillary tangles first appear in the transentorhinal cortex, and then spread to many components of the limbic system, including the thalami, before any signs of dementia are clinically evident. Moreover, a recent MRI diffusion tensor Imaging study [48] has shown significant fractional anisotropy reduction within the thalamus, suggesting changes in the cytoarchitecture within the thalamus and giving further evidence of possible involvement of perturbed corticothalamic and thalamocortical pathways in AD.

As compared to controls, converters showed hypometabolism in the left superior and middle temporal gyri. The lateral surface of the temporal lobe is involved in several cognitive processes, including language and semantic memory processing [49]. In the present study, left temporal lobe hypometabolism appeared to be related to significant impairment of instrumental activities of daily living that marks the conversion from aMCI to AD. MRI studies have shown that the middle and superior temporal gyri are the first neocortical sites to be affected during AD [50], followed by the parietal cortex, at a stage when the frontal lobe is still relatively spared [51]. Karas et al. [52] have reported that AD converters have more left parietal atrophy and left lateral temporal atrophy than stable MCI patients and demonstrated that this site may independently predict conversion. However, in the present study we highlighted hypometabolism but failed to find relative GM reduction in these regions.



The presence of functional but not structural differences between converters and nonconverters in the left temporal lobe was not paralleled by the finding of hypometabolism in converters in comparison to controls. We therefore explored the hypothesis that nonconverters may actually show relatively higher metabolic levels in the left temporal lobe than controls themselves, which was indeed confirmed by statistical analysis (nonconverters versus controls). This unexpected finding points to a possible compensatory mechanism in nonconverters, failure of which would be the underlying pathophysiological correlate of AD conversion. Consistent with this hypothesis, recent papers have suggested a “compensatory response” in stable MCI patients, which fails in those who convert to AD [53, 54]. Moreover, relatively preserved function has been reported even in areas affected by significant atrophy [55]. There are indeed large topographic discrepancies in compensation areas among studies, which could be explained by the different analytical methodologies, intrinsic high variability of compensatory patterns among subjects, and the different severity of disease in the patients under study.

Overall, the present findings suggest that while the posterior cingulate and precuneus show a nearly linear metabolic reduction from normal ageing to AD, functional deficit in other neocortical areas may mark the time of conversion to AD. Specifically, the present results point to the middle and superior temporal gyri, in line with previous findings [15], while other studies have also highlighted the lateral frontal and parietal cortex [56, 57]. Since current results were obtained using rather small groups, studies using wider samples are needed to obtain more robust data that could more clearly depict the regional metabolic failure typical of AD conversion.

In conclusion, the present combined GM VBM and PET VBA investigation showed different patterns of atrophy/hypometabolism in the same group of aMCI patients, either converting to AD or not. The role of posterior cingulate hypometabolism as an early marker of memory deficit was confirmed, while left temporal areas were identified as possible predictors of conversion to AD.

**Acknowledgments** We are grateful to Mr. Michele Chiabrera for assistance with the English editing.

## References

- Petersen RC. Mild cognitive impairment as a diagnostic entity. *J Intern Med.* 2004;256:183–94.
- Feldman HH, Jacova C. Mild cognitive impairment. *Am J Geriatr Psychiatry.* 2005;13:645–55.
- Bennett DA, Wilson RS, Schneider JA, Evans DA, Beckett LA, Aggarwal NT, et al. Natural history of mild cognitive impairment in older persons. *Neurology* 2002;59:198–205.
- Mosconi L, Sorbi S, de Leon MJ, Li Y, Nacmias B, Myoung PS, et al. Hypometabolism exceeds atrophy in presymptomatic early-onset familial Alzheimer’s disease. *J Nucl Med.* 2006;47:1778–86.
- Dubois B, Feldman HH, Jacova C, Dekosky ST, Barberger-Gateau P, Cummings J, et al. Research criteria for the diagnosis of Alzheimer’s disease: revising the NINCDS-ADRDA criteria. *Lancet Neurol.* 2007;6:734–46.
- Price JL, Davis PB, Morris JC, White DL. The distribution of tangles, plaques, and related immunohistochemical markers in healthy aging and Alzheimer’s disease. *Neurobiol Aging.* 1991;12:295–312.
- Gomez-Isla T, Price JL, McKeel DW, Morris JC, Growdon JH, Hyman BT. Profound loss of layer II entorhinal cortex neurons occurs in very mild Alzheimer’s disease. *J Neurosci.* 1996;16:4491–500.
- Jack CR Jr, Petersen RC. Structural imaging approaches to Alzheimer’s disease. In: Scinto LFM, Daffner KR, editors. *Early diagnosis and treatment of Alzheimer’s disease.* Totowa, NJ: Human; 2000. p. 127–48.
- Xu Y, Jack CR Jr, O’Brien PC, Kokmen E, Smith GE, Ivnik RJ, et al. Usefulness of MRI measures of entorhinal cortex versus hippocampus in AD. *Neurology* 2000;54:1760–7.
- Pennanen C, Kivipelto M, Tuomainen S, Hartikainen P, Hanninen T, Laakso MP, et al. Hippocampus and entorhinal cortex in mild cognitive impairment and early AD. *Neurobiol Aging* 2004;25:303–10.
- Chetelat G, Desgranges B, De La Sayette V, Viader F, Eustache F, Baron JC. Mapping grey matter loss with voxel-based morphometry in mild cognitive impairment. *Neuroreport* 2002;13:1939–43.
- Karas GB, Scheltens P, Rombouts SA, Visser PJ, van Schijndel RA, Fox NC, et al. Global and local grey matter loss in mild cognitive impairment and Alzheimer’s disease. *Neuroimage* 2004;23:708–16.
- Mosconi L. Brain glucose metabolism in the early and specific diagnosis of Alzheimer’s disease FDG-PET studies in MCI and AD. *Eur J Nucl Med Mol Imaging* 2005;32:486–510.
- Meguro K, Blaizot X, Kondoh Y, Le Mestric C, Baron JC, Chavoix C. Neocortical and hippocampal glucose hypometabolism following neurotoxic lesions of the entorhinal and perirhinal cortices in the non-human primate as shown by PET. Implications for Alzheimer’s disease. *Brain* 1999;122:1519–31.
- Chetelat G, Desgranges B, De La Sayette V, Viader F, Eustache F, Baron JC. Mild cognitive impairment: can FDG-PET predict who is to rapidly convert to Alzheimer’s disease? *Neurology* 2003;60:1374–7.
- Chetelat G, Desgranges B, de la Sayette V, Viader F, Berkouk K, Landeau B, et al. Dissociating atrophy and hypometabolism impact on episodic memory in mild cognitive impairment. *Brain* 2003;126:1955–67.
- Ishii K, Sasaki H, Kono AK, Miyamoto N, Fukuda T, Mori E. Comparison of grey matter and metabolic reduction in mild Alzheimer’s disease using FDG-PET and voxel-based morphometric MR studies. *Eur J Nucl Med Mol Imaging* 2005;32:959–63.
- Kawachi T, Ishii K, Sakamoto S, Sasaki M, Mori T, Yamashita F, et al. Comparison of the diagnostic performance of FDG-PET and VBM-MRI in very mild Alzheimer’s disease. *Eur J Nucl Med Mol Imaging* 2006;33:801–9.
- Walhovd KB, Fjell AM, Amlien I, Grambaite R, Stenset V, Bjørnerud A, et al. Multimodal imaging in mild cognitive impairment: metabolism, morphometry and diffusion of the temporal-parietal memory network. *Neuroimage* 2009;45(1):215–23.
- Visser PJ, Verhey FR, Boada M, Bullock R, De Deyn PP, Frisoni GB, et al. Development of screening guidelines and clinical criteria for predementia Alzheimer’s disease. The DESCRIPA study. *Neuroepidemiology* 2008;30:254–65.

21. Folstein MF, Folstein SE, McHugh PR. “Mini-Mental State”: a practical method for grading the cognitive state of patients for the clinician. *J Psychiatr Res.* 1975;12:189–98.
22. Katz S, Downs TD, Cash HR, Grotz RC. Progress in development of the index of ADL. *Gerontologist* 1970;10:20–30.
23. Lawton MP, Brody EM. Assessment of older people; self-maintaining and instrumental activities of daily living. *Gerontologist* 1969;9:179–86.
24. Cummings JL, Mega M, Grey K, Rosenberg-Thompson S, Carusi DA, Gornbein J. The Neuropsychiatric Inventory: comprehensive assessment of psychopathology in dementia. *Neurology* 1994;44:2308–14.
25. Masur DM, Fuld PA, Blau AD, Thal LJ, Levin HS, Aronson MK. Distinguishing normal and demented elderly with selective reminding test. *J Clin Exp Neuropsychol* 1989;11:615–30.
26. Carlesimo GA, Caltagirone C, Gainotti G. The Mental Deterioration Battery: normative data, diagnostic reliability and qualitative analysis of cognitive impairment. The group for the standardization of the Mental Deterioration Battery. *Eur Neurol.* 1996;36:378–84.
27. Spinnler H, Tognoni G. Standardizzazione e taratura Italiana di test neuropsicologici. *Ital J Neurol Sci.* 1987;6(Suppl 8):1–120.
28. Barbarotto R, Laiacona M, Frosio R, Vecchio M, Farinato A, Capitani E. A normative study on visual reaction times and two Stroop colour-word tests. *Ital J Neurol Sci.* 1998;19:161–70.
29. Watson YI, Arfken CL, Birge SJ. Clock completion: an objective screening test for dementia. *J Am Geriatr Soc.* 1993;41:1235–40.
30. Amodio P, Wenin H, Del Piccolo F, Mapelli D, Montagnese S, Pellegrini A, et al. Variability of trail making test, symbol digit test and line trait test in normal people. A normative study taking into account age-dependent decline and sociobiological variables. *Aging Clin Exp Res.* 2002;14:117–31.
31. McKhann G, Drachman D, Folstein M, Katzman R, Price D, Stadlan EM. Clinical diagnosis of Alzheimer’s disease: report of the NINCDS-ADRDA Work Group under the auspices of Department of Health and Human Services Task Force on Alzheimer’s Disease. *Neurology* 1984;34:939–44.
32. Bartenstein P, Asenbaum S, Catafau A, Halldin C, Pilowski L, Pupi A, et al. European Association of Nuclear Medicine procedure guidelines for brain imaging using [(18)F]FDG. *Eur J Nucl Med.* 2002;29:BP43–8.
33. Talairach J, Tournoux P. Co-planar stereotaxic atlas of the human brain. New York: Thieme Medical; 1988.
34. Friston KJ, Holmes AP, Worsley KJ, Poline JP, Frith CD, Frackowiak RSJ. Statistical parametric maps in functional imaging: a general linear approach. *Hum Brain Mapp.* 1994;2:189–210.
35. Gispert JD, Pascau J, Reig S, Martínez-Lázaro R, Molina V, García-Barreno P, et al. Influence of the normalization template on the outcome of statistical parametric mapping of PET scans. *Neuroimage* 2003;19:601–12.
36. Meyer JH, Gunn RN, Myers R, Grasby PM. Assessment of spatial normalization of PET ligand images using ligand-specific templates. *Neuroimage* 1999;9:545–53.
37. Good CD, Johnsrude IS, Ashburner J, Henson RN, Friston KJ, Frackowiak RS. A voxel-based morphometric study of ageing in 465 normal adult human brains. *Neuroimage* 2001;14:21–36.
38. Oishi N, Udaka F, Kameyama M, Sawamoto N, Hashikawa K, Fukuyama H. Regional cerebral blood flow in Parkinson disease with nonpsychotic visual hallucinations. *Neurology* 2005;65:1708–15.
39. Nestor PJ, Fryer TD, Smielewski P, Hodges JR. Limbic hypometabolism in Alzheimer’s disease and mild cognitive impairment. *Ann Neurol.* 2003;54:343–51.
40. Kogure D, Matsuda H, Ohnishi T, Asada T, Uno M, Kunihiko T, et al. Longitudinal evaluation of early Alzheimer’s disease using brain perfusion SPECT. *J Nucl Med.* 2000;41:1155–62.
41. Caroli A, Testa C, Geroldi C, Nobili F, Barnden LR, Guerra UP, et al. Cerebral perfusion correlates of conversion to Alzheimer’s disease in amnesic mild cognitive impairment. *J Neurol.* 2007;254:1698–707.
42. Mitchell AJ, Shiri-Feshki M. Temporal trends in the long term risk of progression of mild cognitive impairment: a pooled analysis. *J Neurol Neurosurg Psychiatry* 2008;79(12):1386–91.
43. de Leon MJ, George AE, Stylopoulos LA, Smith G, Miller DC. Early marker for Alzheimer’s disease: the atrophic hippocampus. *Lancet* 1989;2:672–3.
44. Braak H, Braak E. Evolution of the neuropathology of Alzheimer’s disease. *Acta Neurol Scand Suppl.* 1996;165:3–12.
45. Magistretti PJ. Cellular basis of functional brain imaging: insight from neural-glia metabolic coupling. *Brain Res.* 2000;886:108–12.
46. Price JL, Morris JC. Tangles and plaques in nondemented aging and “preclinical” Alzheimer’s disease. *Ann Neurol.* 1999;45:358–68.
47. Callen DJA, Black SE, Gao F, Caldwell CB, Szalai JP. Beyond the hippocampus: MRI volumetry confirms widespread limbic atrophy in AD. *Neurology* 2001;57:1669–74.
48. Rose SE, Janke AL, Chalk JB. Grey and white matter changes in Alzheimer’s disease: a diffusion tensor imaging study. *J Magn Reson Imaging* 2008;27:20–6.
49. Cabeza R, Nyberg L. Imaging cognition, II: an empirical review of 275 PET and fMRI studies. *J Cogn Neurosci.* 2000;12:1–47.
50. Convit A, de Asis J, de Leon MJ, Tarshis CY, De Santi S, Rusinek H. Atrophy of the medial occipitotemporal, inferior, and middle temporal gyri in non-demented elderly predict decline to Alzheimer’s disease. *Neurobiol Aging* 2000;21(1):19–26.
51. Whitwell JL, Przybelski SA, Weigand SD, Knopman DS, Boeve BF, Petersen RC, et al. 3D maps from multiple MRI illustrate changing atrophy patterns as subjects progress from mild cognitive impairment to Alzheimer’s disease. *Brain* 2007;130:1777–86.
52. Karas G, Sluimer J, Goekoop R, van der Flier W, Rombouts SA, Vrenken H, et al. Amnesic mild cognitive impairment: structural MR imaging findings predictive of conversion to Alzheimer disease. *AJNR Am J Neuroradiol* 2008;29(5):944–9.
53. Hunt A, Schönknecht P, Henze M, Seidl U, Haberkorn U, Schröder J. Reduced cerebral glucose metabolism in patients at risk for Alzheimer’s disease. *Psychiatry Res.* 2007;155:147–54.
54. Nobili F, Salmaso D, Morbelli S, Girtler N, Piccardo A, Brugnolo A, et al. Principal component analysis of FDG PET in amnesic MCI. *Eur J Nucl Med Mol Imaging* 2008;35:2191–202.
55. Caroli A, Geroldi C, Nobili F, Barnden LR, Guerra UP, Bonetti M, et al. Functional compensation in incipient Alzheimer’s disease. *Neurobiol Aging* 2008. doi:10.1016/j.neurobiolaging.2008.05.001
56. Mosconi L, Perani D, Sorbi S, Herholz K, Nacmias B, Holthoff V, et al. MCI conversion to dementia and the APOE genotype: a prediction study with FDG-PET. *Neurology* 2004;63:2332–40.
57. Anchisi D, Borroni B, Franceschi M, Kerrouche N, Kalbe E, Beuthien-Beumann B, et al. Heterogeneity of brain glucose metabolism in mild cognitive impairment and clinical progression to Alzheimer disease. *Arch Neurol.* 2005;62:1728–33.